

Side-leakage of facemask

B.N.J. Persson^{1,2}

¹*PGI-1, FZ Jülich, Germany, EU*

²*www.MultiscaleConsulting.com*

Face masks are used to trap particles (or fluid drops) in a porous material (filter) in order to avoid or reduce the transfer of particles between the human lungs (or mouth and nose) and the external environment. The air exchange between the lungs and the environment is assumed to occur through the facemask filter. However, if the resistance to air flow through the filter is high some air (and accompanied particles) will leak through the filter-skin interface. In this paper I will present a model study of the side-leakage problem.

1 Introduction

Face masks are used to trap particles in a porous material (filter) in order to avoid or reduce the transfer of particles between the human lungs and the external environment[1]. The filter usually consist of a sheet of randomly arranged fibers made from a polymer, e.g. polyethylene. The effectiveness of the filter will increase with increasing thickness of the filter and with decreasing size of the open channels through the filter. However, increasing the effectiveness of the filter will in general increase the resistance to the air flow through the filter, which may result in uncomfortable breathing experience, or side leakage of air between the skin and the filter surface. Thus, a recent report demonstrates the potential risk of increased face-to-mask seal leakage when N95 filtering facepiece respirators (N95 FFR) are covered by surgical, cloth, or medical masks[2]. In this paper I will present a more detailed model study of the side-leakage problem.

2 Theory

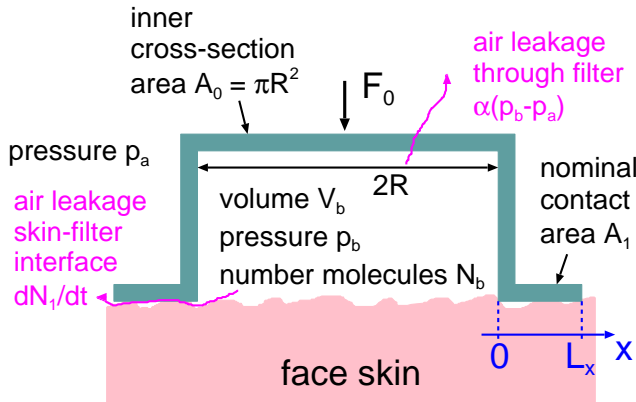


FIG. 1. Model used for studying the air flow for facemask. The air can flow through the filter at a number flow rate $\alpha'(p_b - p_a)$ or at the interface between the skin and the facemask at a number flow rate $dN_1/dt = \dot{N}_1$. The number of air molecules N_b and the air pressure p_b in the volume V_b between the facemask and the face varies in time due to the breathing act.

We consider the simplest (idealized) case where the facemask makes contact with the skin over a circular annulus (radius R) of width L_x in the radial (air leakage) direction and $L_y = 2\pi R$ in the orthogonal angular direction (see Fig. 1). We assume the nominal contact pressure is constant in the nominal contact area $A_1 = L_x L_y$. The air volume between the face and the facemask is denoted by V_b and is assumed to be constant. The facemask is pushed against the skin by a force F_0 given by the extension of the rubber band, which is used to attach the facemask to the head, and with the force $A_0(p_b - p_a)$ due to the air pressure difference between inside and outside the mask. The spring contact pressure $p_s = F_0/A_1$. The nominal contact pressure in the area A_1 is

$$p = p_s - \beta(p_b - p_a), \quad (1)$$

where

$$\beta = A_0/A_1 + \beta',$$

where p_b is the air pressure inside the facemask and p_a the air pressure outside, which is assumed to be constant and equal to 1 atm (1 bar). The factor β' is a number between 0.5 and 1 which depends on how the air pressure change from p_b at $x = 0$ to p_a at $x = L_x$ (see Fig. 1). Since $A_0/A_1 = \pi R^2/(2\pi R L_x) = R/2L_x$ we have $\beta = R/2L_x + \beta'$. For N95 masks the contact width L_x is relative small so that $R/2L_x \gg 1$ and β' is not so important.

The number of air molecules $N_b(t)$ inside the facemask satisfies

$$\dot{N}_b = \dot{N}(t) - \alpha'(p_b - p_a) - \dot{N}_1 \quad (2)$$

where \dot{N} is the number of air molecules entering the volume V_b from the lungs, and $\alpha'(p_b - p_a)$ the number of air molecules leaking through the facemask filter and \dot{N}_1 the number of air molecules leaking between the skin and the facemask, which depends on the nominal contact pressure p and the pressure difference $\Delta p = p_b - p_a$ between inside and outside. We will assume the ideal gas law so that

$$p_b V_b = N_b k_B T \quad (3)$$

The leakrate \dot{N}_1 is given approximately by[3, 4]

$$\dot{N}_1 = \frac{1}{24} \frac{L_y}{L_x} \frac{(p_b^2 - p_a^2) u_c^3}{k_B T \eta} \quad (4)$$

Here $k_B T$ is the thermal energy (k_B is the Boltzmann constant and T the absolute temperature), and u_c is an effective surface separation which we determine using the Persson contact mechanics theory[5–7] and the Brugge-man effective medium theory as described elsewhere[8–11].

The gas viscosity

$$\eta = \frac{1}{3} m n \bar{v} \lambda$$

where n is the gas number density and λ the mean free path due to collisions between gas molecules. Note that $\lambda \sim 1/n$ so the viscosity η is independent of the gas number density. Equations (1)-(4) are 4 equations for the 4 unknown quantities, p , p_b , N_b and N_1 .

We denote the resistance to air flow through the face-mask filter by $1/\alpha$, where the air flow conductance α is defined by

$$\frac{dV}{dt} = \alpha(p_b - p_a)$$

where $\dot{V} = dV/dt$ is the volume of air of atmospheric pressure passing through the facemask filter per unit time given the pressure difference $\Delta p = p_b - p_a$ between inside and outside the facemask. Using the ideal gas law we have

$$p_a \dot{V} = \dot{N} k_B T = \alpha'(p_b - p_a) k_B T$$

so that $\alpha = \alpha' k_B T / p_a$.

3 Numerical results

We will assume that air molecules is injected and removed from the volume V_b by the breathing action in a periodic way so that

$$N(t) = N_0 \sin(\omega_0 t)$$

corresponding to a volume of air (of atmospheric pressure) $V(t) = k_B T N(t) / p_a$,

$$V(t) = V_0 \sin(\omega_0 t)$$

where $\omega_0 = 2\pi/T$ where T is the period of breathing. We assume that at time $t = 0$, $p_b = p_a$ and hence from (4), $\dot{N}_1 = 0$ for $t = 0$.

Ref. [12] present the air flow conductance of several types of facemasks. For the US N95 facemask for the air flow $\dot{V} = 85$ liter/min the pressure difference $p_b - p_a$ should be smaller than 343 Pa during inhalation and 245 Pa during exhalation (the two pressure drops may differ because of side leakage). If the leakage would be entirely through the facemask these two cases correspond to $\alpha \approx 0.25$ and $\alpha \approx 0.35$ liter/min \cdot Pa. For the European FFP2 facemask slightly larger (minimum) flow conductance are required. Below we show results for $\alpha = 0.3$ and 0.15 liter/min \cdot Pa, where the smaller value may reflect a N95 facemask contaminated by particles which block air flow channels.

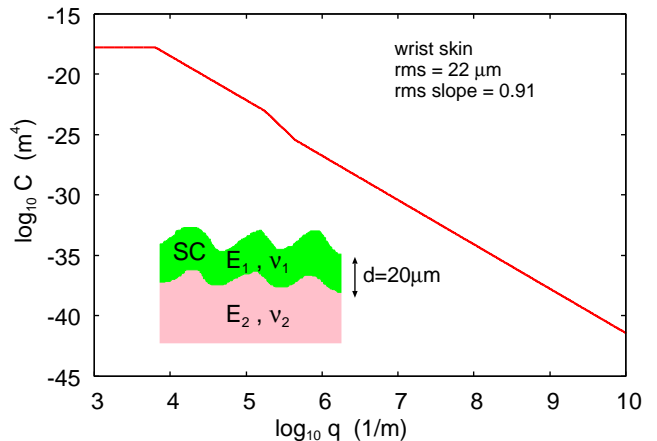


FIG. 2. The surface roughness power spectrum as a function of the wavenumber (log-log scale) obtained from optical and AFM measurements of the surface topography of the wrist skin of a 49 years old man (from Ref. [13, 14]). The surface has the rms roughness amplitude $22 \mu\text{m}$ and the rms slope 0.91. The inset shows the skin model used in the contact mechanics model calculations. The Young's modulus and Poisson ratio of the top layer of the skin (stratum corneum, of thickness $d = 20 \mu\text{m}$) are $E_1 = 1$ GPa and $\nu_1 = 0.5$, while the material below the top layer has $E_2 = 20$ kPa and $\nu_2 = 0.5$ (see [16] for information about the human skin elastic properties).

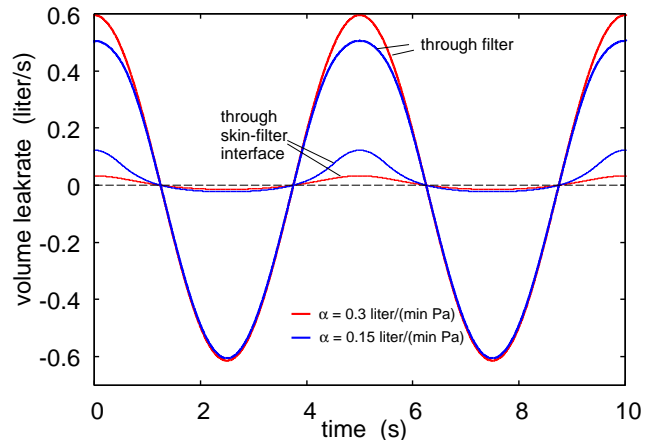


FIG. 3. The air (of atmospheric pressure) volume leak rate in liter/s as a function of time during breathing at the period of $T = 5$ sec and the volume $V_0 = 0.5$ liter: $V(t) = V_0 \sin(\omega t)$ with $\omega = 2\pi/T$. The red and blue curves are for the filter air flow conductance $\alpha = 0.3$ and 0.15 liter/(min \cdot Pa). The thick lines is the leakage through the filter and the thinner lines at the skin-filter interface.

In the numerical study we use $T = 5$ s and $V_0 = 0.5$ liter, corresponding to an air volume 1 liter oscillating between the lungs and the outside of the lungs. We use the spring force $F_0 = 3$ N as measured for a N95 facemask on my head. The facemask is assumed to make (nominal) contact with the skin over a circular strip of with $L_x = 3$ mm in the (radial) air leakage direction and

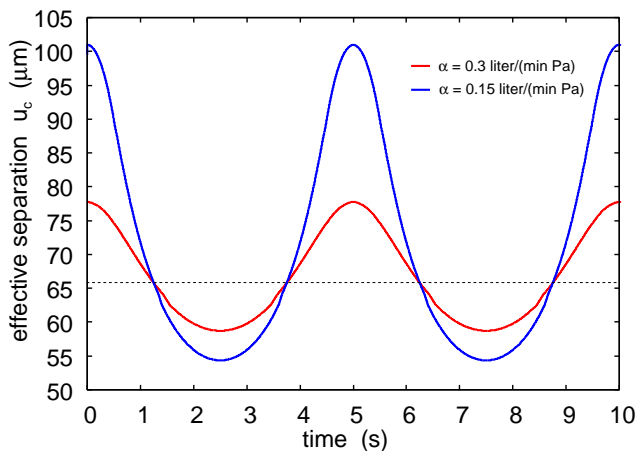


FIG. 4. The effective surface separation as a function of time.

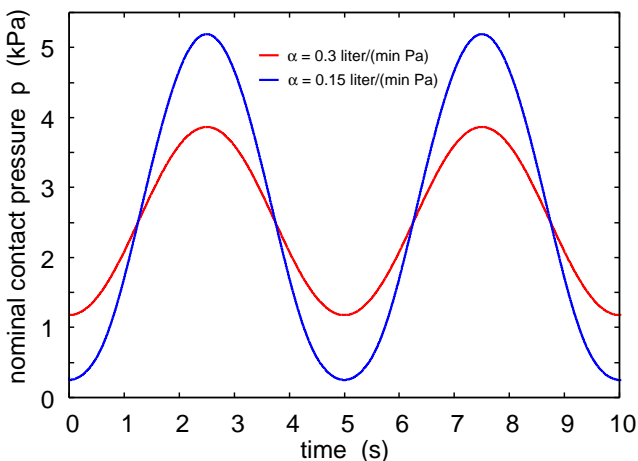


FIG. 5. The nominal contact pressure in the filter-skin nominal contact area, as a function of time.

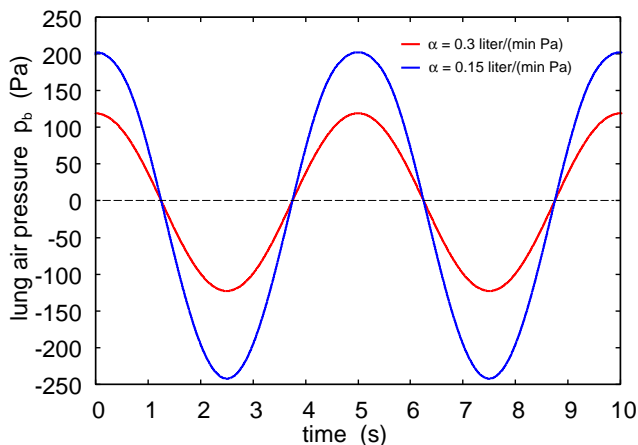


FIG. 6. The air pressure (relative to the atmospheric pressure) in the lungs as a function of time.

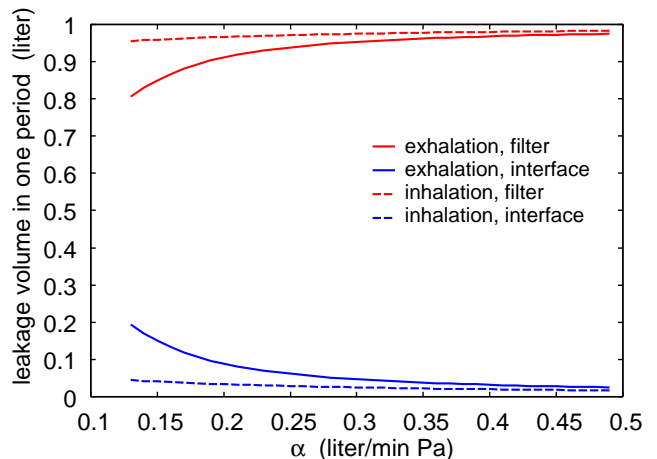


FIG. 7. The volume of air passing through the filter (red lines) and through the skin-filter interface (blue lines) as a function of the filter air flow conductance. The solid lines are during exhalation and the dashed lines during inhalation.

of length $L_y = 2\pi R = 40$ cm is the orthogonal angular direction. The volume between the face and the facemask is assumed to be constant in time and equal to 0.1 liter. In reality the volume will fluctuate in time due to the oscillations in the air pressure $p_b(t)$, but this effect is not very important.

To calculate the air side leakage it is necessary to know the surface roughness on the facemask and the skin in the nominal contact region. Here we will use the surface roughness measured on the wrist skin in Ref. [13, 14]. We expect the roughness on the skin on the face to be similar but we have not studied it. We note, however, that if the skin is covered by hair (beard, poorly shaved or unshaved) this could effectively strongly increase the surface roughness and result in much larger leakage rates than predicted below[15]. In this section we will assume that the facemask surface has no surface roughness. Including the surface roughness on the facemask surface will increase the side leakage.

Fig. 2 shows the surface roughness power spectrum as a function of the wavenumber (log-log scale) obtained from optical and AFM measurements of the surface topography of the wrist skin of a 49 years old man (from Ref. [13, 14]). The surface has the root-mean-square (rms) roughness amplitude $22 \mu\text{m}$ and the rms slope 0.91. The inset shows the skin model used in the contact mechanics model calculations. The Young's modulus and Poisson ratio of the top layer of the skin (stratum corneum, of thickness $d = 20 \mu\text{m}$) are $E_1 = 1$ GPa and $\nu_1 = 0.5$, while the material below the top layer has $E_2 = 20$ kPa and $\nu_2 = 0.5$ (see [16] for information about the human skin elastic properties).

Fig. 3 shows the air (of atmospheric pressure) volume leak rate in liter/s as a function of time during breathing. The red and blue curves are for the filter air flow conduc-

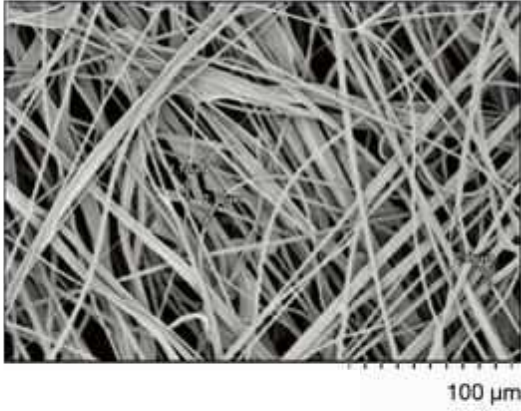


FIG. 8. Scanning electron micrograph image of filter layer (non-woven polypropylene, melt blown). Adapted from Ref. [17].

tance $\alpha = 0.3$ and 0.15 liter/(min · Pa). The thick lines is the leakage through the filter and the thinner lines at the skin-filter interface. Note that the side air leakage is larger during exhalation than during inhalation. This is due to the air pressure term $(p_b - p_a)A_0$ which increases the force squeezing the facemask against the skin during inhalation while it reduces the contact force during exhalation. For $\alpha = 0.3$ liter/(min · Pa) for exhalation about 5% of the air leaks between the skin and the facemask while during inhalation only 2.6% of the air side leaks. For $\alpha = 0.15$ liter/(min · Pa) the corresponding numbers are 18% and 4%.

Fig. 4 shows the effective surface separation u_c as a function of time. The dotted line indicate the effective surface separation when there is no pressure force, i.e., when $p_a = p_b$. As expected, during exhalation the surface separation increases while it decreases during inhalation. Similarly, the nominal contact pressure in the filter-skin nominal contact area decreases during exhalation and increases during inhalation as shown in Fig. 5. Fig. 6 shows the air pressure (relative to the atmospheric pressure) in the facemask volume V_b as a function of time.

Finally, in Fig 7 we show the volume of air passing through the filter (red lines) and through the skin-filter interface (blue lines) as a function of the filter air flow conductance. The solid lines is during exhalation and the dashed lines during inhalation. For small air filter conductance the side leakage is large during exhalation while during inhalation there is a much smaller side leakage.

4 Discussion

The study above is very idealized as we have assumed a uniform contact pressure in the facemask-skin nominal contact area. We have also neglected the surface roughness on the facemask and treated the facemask as rigid when calculating the effective surface separation u_c which determined the leakrate.

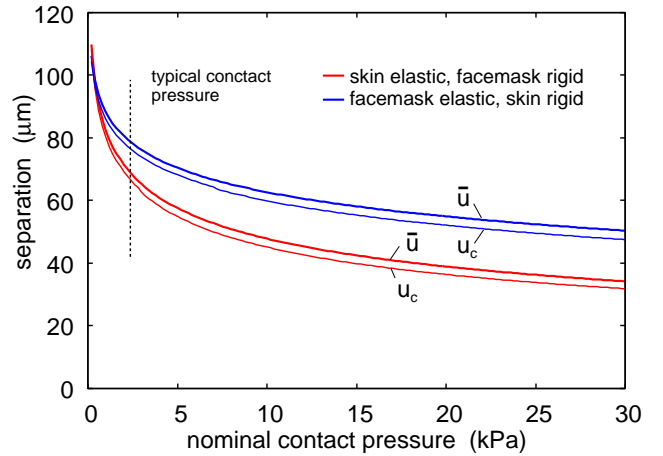


FIG. 9. The average interfacial separation \bar{u} , and the separation u_c which determines the air leakage [see (4)], as a function of the nominal contact pressure. The red lines are the results assuming the facemask is rigid and the skin elastic (with layered elastic properties, see Fig. 2), and the blue lines is the result assuming the facemask elastic (with thickness 1 mm and with $E = 27.5$ MPa and $\nu = 0.37$) and the skin rigid. Only the surface roughness of the skin (with the power spectrum shown in Fig. 2) is included in the calculations.

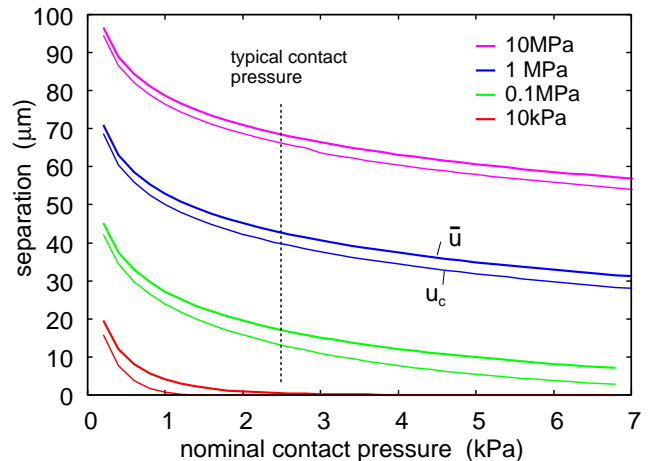


FIG. 10. The average interfacial separation \bar{u} , and the separation u_c which determines the air leakage [see (4)], as a function of the nominal contact pressure. Results are shown for the elastic modulus $E = 10, 1, 0.1$ and 0.01 MPa. In all cases the Poisson ratio $\nu = 0.5$. Only the surface roughness of the skin (with the power spectrum shown in Fig. 2) is included in the calculations.

The N95 facemask is built from non-woven polymer fibers, e.g., polypropylene, polyethylene or polyesters (see Fig. 8)[1]. (Recently it has been suggested to instead use polymer films with a periodic distribution of closely spaced nanoholes as facemask filters[18].) The polymers have a large elastic modulus (typically several GPa) but the fiber mat is macroscopically soft with an effective modulus in tension typically in the range

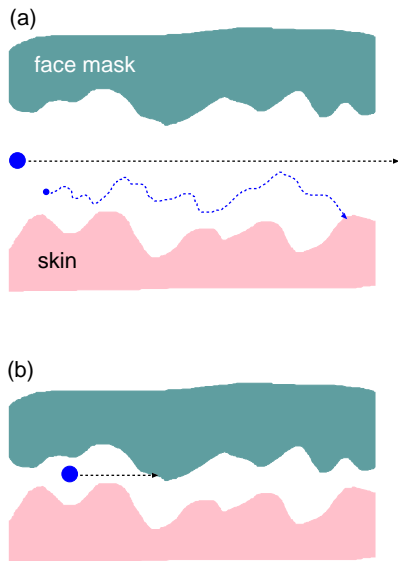


FIG. 11. A large particle or droplet, due to its large inertia, will not be able to respond to the rapidly fluctuating (due to the surface roughness) air flow current and will hence move through the skin-filter nominal contact region on a nearly straight line. (a) If the average spacing between the surfaces in the air flow channels are much larger than the surface roughness amplitude then big particles may pass through the contact without collisions with the walls. (b) If the average spacing is of order, or smaller than, the surface roughness amplitude the big particle is likely to hit into the solid walls. A very small particle will perform Brownian motion in addition to drifting with the air flow. In this case if the Brownian motion amplitude is big enough the particle may hit into a wall even if the average wall separation is large as in (a).

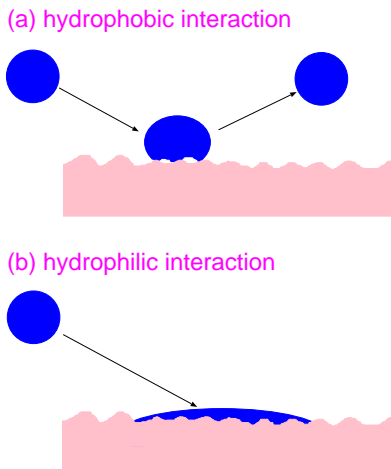


FIG. 12. (a) If the fluid-solid interaction is hydrophobic a liquid droplet hitting a solid may bounce off without transfer of fluid to the solid wall[26, 27]. (b) If the interaction is hydrophilic the droplet may be adsorbed on the solid wall.

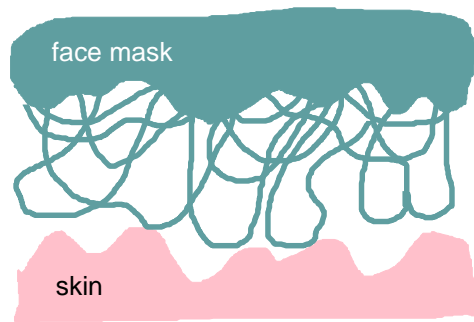


FIG. 13. The N95 mask has a thin layer of fibers pointing away from the facemask surface which may help to trap particles in the side leakage air flow channel.

10–100 MPa. The fiber mat can be treated as an homogeneous material only on length scales larger than both the fiber width (or thickness), and the average distance between two nearby fiber segments which typically means distances of order $10 \mu\text{m}$ or more. However, because of the low nominal contact pressure, the average and effective surface separation in the present case are determined by the most long wavelength surface roughness components so to a good approximation we can treat the fiber mat as a homogeneous material. Another problem is that the fiber mat cannot in general be treated as a isotropic elastic material but the effective modulus E_z which determine the elongation (tension) normal to the film, which is important for the contact mechanics, may differ from the elastic modulus $E_x = E_y$ in tension within the film plane. However, if the fibers bind to each other where they touch each other, and if they are closely spaced, we expect the effective modulus E_z to be similar to the modulus in tension within the plane.

We now show that including the macroscopic elastic properties of the facemask material, by using the modulus obtained in tension, will not result in any drastic change in the results presented above. To illustrate this, in Fig. 9 we show the average interfacial separation \bar{u} , and the separation u_c which determines the air leakage [see (4)], as a function of the nominal contact pressure. The red lines are the results assuming the facemask is rigid and the skin elastic (with layered elastic properties, see Fig. 2), and the blue lines is the result assuming the facemask elastic (with $E_x = 27.5 \text{ MPa}$ and $\nu = 0.37$, as measured for non-woven polypropylene in tension[19, 20]) and the skin rigid. In the latter case we have assumed the facemask has the thickness 1 mm but practically the same result is obtained assuming infinite thickness. Only the surface roughness of the skin (with the power spectrum shown in Fig. 2) is included in the calculations.

We will show below that in order to effectively trap particles and droplets the surface separation in the nominal skin-facemask contact region should be much smaller than shown in Fig. 9. This can be realized if the rim

of the facemask is covered by a strip of a soft material, e.g., weakly crosslinked Polydimethylsiloxan (PDMS). To illustrate what elastic modulus is necessary, in Fig. 10 we show the average interfacial separation \bar{u} , and the separation u_c which determines the air leakage [see (4)], as a function of the nominal contact pressure. Results are shown for the elastic modulus $E = 10, 1, 0.1$ and 0.01 MPa. In all cases the Poisson ratio $\nu = 0.5$. Only the surface roughness of the skin (with the power spectrum shown in Fig. 2) is included in the calculations. Note that for $E < 10$ kPa the contact area percolate at a pressure below the average pressure in the skin-facemask contact region, so for such soft material no leakage of air or particles would be possible. In the calculations we have neglected adhesion which is important for the leakage only for very soft materials with $E < 0.1$ MPa (see Appendix A). Thus including adhesion for the $E = 10$ kPa case in Fig. 10 would reduce \bar{u} and u_c .

A weakly crosslinked PDMS would be very sticky and perhaps uncomfortable to use and may get contaminated by dust particles. Another possibility would be to use an elastically soft hydrogel[21, 22] strip at the edge of the facemask, with a thickness of order a few mm. A proper chosen hydrogel may exhibit no or negligible adhesion to the human skin[23]. However, hydrogels will dehydrate and becomes rigid in air but perhaps the moisture in the air from the lungs is enough to keep it hydrated.

So far we have only considered the air flow problem. The question is now if particles in the air are able to follow the air flow into or out of the facemask volume V_b . For the flow through the facemask filter this problem has been studied in detail both theoretically and experimentally. Several different mechanisms have been proposed which result in trapping of particles in the filter:

(A) Inertial Impacting: Aerosol or dust particles typically $1 \mu\text{m}$ or larger in size with enough inertia to prevent them from flowing around the fibers in the filtration layers slam into the mask material where they may adhere (but see below) and get filtered.

(B) Diffusion: Particles smaller than $1 \mu\text{m}$, usually $0.1 \mu\text{m}$ and smaller that are not subject to inertia undergo diffusion and get stuck to fibrous layers of the filter while undergoing Brownian motion around the tortuous porous matrix of the filter fiber.

(C) Electrostatic attraction: This mechanism employs electrocharged polymer or resin fibers that attract both large and small oppositely charged particles, or neutral particles via polarization (induced dipole) effects, and trap them. This effect depends on the distribution of positive and negative charges on the polymer surfaces (the total charge is likely to vanish so there must be an equal number of positive and negative charges on the polymer fibers)[24].

The critical or equivalent pore diameter (see Appendix B and Ref. [25]) in currently available N95 masks are around 300 nm in size, while the SARS-CoV-2 virus is

significantly smaller at 65 to 125 nm . However, the virus always travels attached to larger particles that are consistently snared by the filter. Thus, the virus are usually attaches to water droplets or aerosols (i.e. really small droplets) that are generated by breathing, talking, coughing, etc. These consist of water, mucus protein and other biological material and are all of order or larger than $1 \mu\text{m}$. And even if the particles were smaller than the N95 filter size, the erratic Brownian motion of particles that size and the electrostatic attraction generated by the mask means they would be consistently caught as well.

The fibers in facemasks are usually made from a hydrophobic polymer in order to avoid the facemask absorb moisture from the air from the lungs. However, experiments have shown that a water droplet hitting a hydrophobic surface may bounce off which would result in a reduced trapping of fluid (aerosols) droplets (see Fig. 12)[26, 27]. Thus an interesting problem is to find out which water contact angle is optimal in order to avoid (or reduce) water absorption from the humid air from the lungs but still allow water droplets to get stuck to the fibers during impact from the air. Once stuck to a fiber it is also important what happens to a respiratory droplet (e.g. evaporation of water) as this may effect the time period a trapped virus (or bacteria) is intact or alive[28]. This too will depend on the chemical nature (and the surface topography) of the fiber material.

The N95 and FFP2 facemasks have thin layers of fibers pointing away from the facemask surfaces which may help to trap particles in the side leakage air flow channel (see Fig. 13).

Experiments have shown that N95 masks are actually best for particles either larger or smaller than the 300 nm threshold. Thus N95 masks actually have that name because they are 95% efficient at stopping particles in their least efficient particle size range in this case those around $0.3 \mu\text{m}$. Thus, particles smaller than $\sim 1 \mu\text{m}$ perform erratic, zig-zagging Brownian motion with large enough amplitude to hit into a fiber, which greatly increases the chance they will be snared by the mask fibers.

The trapping mechanisms (A)-(C) are also relevant for trapping if particles in the air stream between the skin and the facemask. However, the effective separation between the skin and the facemask is much larger than the $0.3 \mu\text{m}$ pore size in the facemask filter. Thus Fig. 4 shown that u_c is typically between $50 - 100 \mu\text{m}$ which is several times bigger than the skin rms roughness amplitude (about $20 \mu\text{m}$). Hence it is possible for micrometer sized particles to pass through the skin-facemask contact region as indicated in Fig. 11(a). In order for the inertia effect trapping mechanism to be effective one would need the average surface separation to be of order the rms surface roughness amplitude as indicated in Fig. 11(b). Furthermore, the Brownian motion trapping mechanism (B) (see Fig. 11(a)) may be ineffective to trap small

particles. To see this note that during a time t the mean square displacement, due to Brownian motion of a spherical particle (radius R), in one direction is given by[29]

$$\langle x^2 \rangle = \frac{k_B T t}{3\pi\eta R} \quad (5)$$

The (average) air flow velocity v in the skin-facemask interfacial region is given by $\dot{V} = vL_y\bar{u}$ where \dot{V} is the volume rate of air leakage at the interface and \bar{u} the average surface separation. Using $\dot{V} = 0.03$ liter/s and $\bar{u} = 70$ μm gives $v \approx 1$ m/s. We assume the Brownian particle drift with the air stream so the time in the interfacial region will be $t = L_x/v$ or $t \approx 3 \times 10^{-3}$ s where we have used $L_x = 3$ mm. Using the air viscosity $\eta \approx 2 \times 10^{-5}$ Pas and $\langle x^2 \rangle \approx \bar{u}^2$ we get

$$R \approx \frac{k_B T t}{3\pi\eta\bar{u}^2} \approx 10^{-11} \text{ m}$$

Thus, trapping of particles resulting from Brownian motion is negligible in the side leakage channel. This is different in the facemask filter where the open channels may on the average have a diameter of order 1 μm (and the most narrow constriction may be only 0.3 μm). This will enhance R by a factor $(70/1)^2 \approx 5000$ which will make Brownian motion important for particles smaller than ~ 0.1 μm .

5 Summary and conclusion

We have studied a very simple model for the side leakage of facemasks. We have assumed that the skin-facemask nominal contact pressure is the same everywhere in the nominal contact area, and neglected the surface roughness of the facemask surface. The calculations indicate that under normal conditions for the N95 or FFP2 facemasks a few % of the air may leak through the skin-facemask interface. The average separation between the surfaces in the skin-facemask contact region is much larger than the effective pore size in the facemask filter which allow suspended particles in the air to enter or leave the facemask volume V_b during inhalation and exhalation.

Acknowledgments:

I thank J.P. Gong, M. Scaraggi and E. Tosatti for useful comments on the manuscript.

Appendix A: role of adhesion

In calculating the air leakrate we have used the effective medium approach combined with the Persson contact mechanics theory for the probability distribution of surface separations. The basic contact mechanics picture (critical junction theory) which can be used to estimate the leak-rate of seals is as follows: Consider first a seal where the nominal contact area is a square. The seal separate a high-pressure gas on one side from a low pressure gas on the other side, with the pressure drop

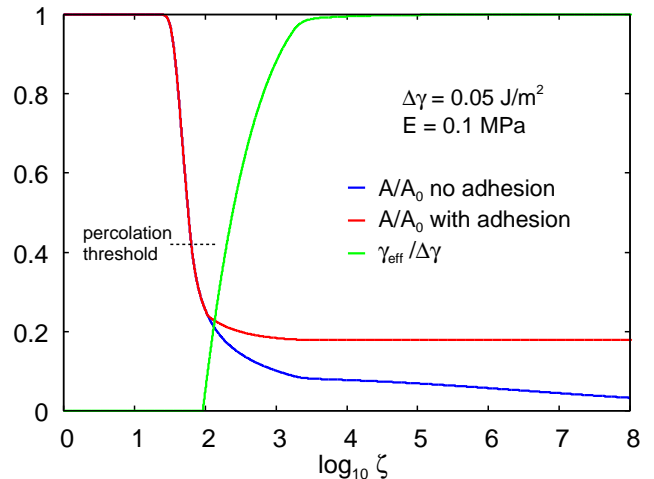


FIG. 14. The relative contact area A/A_0 with (red line) and without (blue line) adhesion, and the effective interfacial binding energy γ_{eff} (or work of adhesion) (green line) as a function of the logarithm of the magnification. We have used the elastic modulus $E = 0.1$ MPa and the work of adhesion for smooth surfaces $\Delta\gamma = 0.05$ J/m². Note that the contact area percolate at a magnification where the adhesion does not manifest itself.

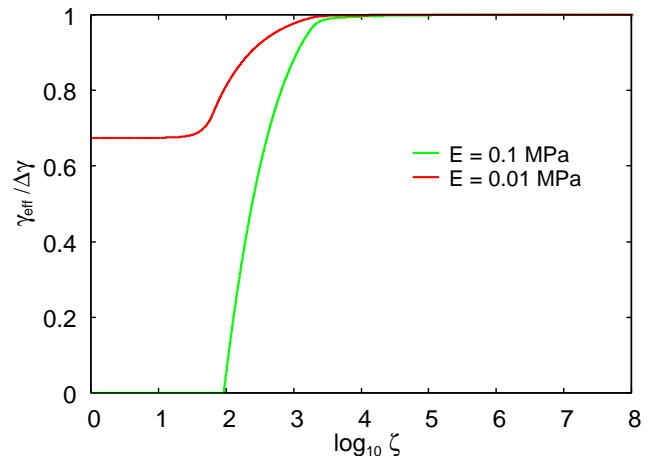


FIG. 15. The effective interfacial binding energy γ_{eff} (or work of adhesion) as a function of the logarithm of the magnification. We have used the elastic modulus $E = 0.1$ MPa (green line) and $E = 0.01$ MPa (red line), and the work of adhesion for smooth surfaces $\Delta\gamma = 0.05$ J/m². Note that γ_{eff} vanish for $\zeta = 1$ when $E = 0.1$ MPa while it is nonzero when $E = 0.01$ MPa. Thus only in the latter case will there be a finite pull-off force in the adiabatic (infinitely slowly) pull-off limit.

ΔP . We consider the interface between the solids at increasing magnification ζ . At the magnification ζ only roughness components with wavenumber $q < \zeta q_0$ can be observed, where q_0 is the smallest wavenumber. At low magnification we observe no surface roughness and it appears as if the contact is complete (see blue line in Fig. 14). Thus studying the interface only at this low

magnification we would be tempted to conclude that the leak-rate vanishes. However, as we increase the magnification ζ we observe surface roughness and non-contact regions, so that the contact area $A(\zeta)$ is smaller than the nominal contact area $A_0 = A(1)$. As we increase the magnification further, we observe shorter wavelength roughness, and $A(\zeta)$ decreases further. For randomly rough surfaces, as a function of increasing magnification, when $A(\zeta)/A_0 \approx 0.42$ the non-contact area percolate[8], and the first open channel is observed, which allow fluid to flow from the high pressure side to the low pressure side. The percolating channel has a most narrow constriction over which most of the pressure drop ΔP occur. In the simplest picture one assume that the whole pressure drop ΔP occur over this *critical constriction*, and if it is approximated by a rectangular pore of height u_c much smaller than its width w (as predicted by contact mechanics theory), the leak rate can be approximated by Eq. (4). The height u_c of the critical constriction can be obtained using the Persson contact mechanics theory (see Ref. [5–7]).

When adhesion is included the average interfacial separation \bar{u} and u_c decreases. However, the influence of adhesion on these quantities is in the present case negligible when the elastic modulus $E > 0.1$ MPa. This can be understood by studying how the contact area decreases with the magnification. Fig. 14 shows the relative contact area A/A_0 with (red line) and without (blue line) adhesion, and the effective interfacial binding energy γ_{eff} (or work of adhesion) (green line) as a function of the logarithm of the magnification[30, 31]. We have used the elastic modulus $E = 0.1$ MPa and the work of adhesion for smooth surfaces $\Delta\gamma = 0.05$ J/m² (as typical for adhesion involving PDMS). Note that the contact area percolate at a magnification where the adhesion does not manifest itself.

Fig. 15 shows the effective interfacial binding energy γ_{eff} (or work of adhesion) as a function of the logarithm of the magnification. We have used the elastic modulus $E = 0.1$ MPa (green line) and $E = 0.01$ MPa (red line), and the work of adhesion for smooth surfaces $\Delta\gamma = 0.05$ J/m². Note that γ_{eff} vanish for $\zeta = 1$ when $E = 0.1$ MPa while it is nonzero for $\zeta = 1$ when $E = 0.01$ MPa. Thus only in the latter case will there be a finite pull-off force in the adiabatic (infinitely slowly) pull-off limit.

We note finally that for some hydrogel–countersurface systems it is possible to avoid adhesion[23], in particular at the low contact pressures of interest here. The effective repulsion in these systems is an entropy effect related to squeezing out water from the interface resulting in a higher concentration of the solvated ions in the water, which screen surface charges bound to the gel surface.

Appendix B: effective pore size

Filters made from non-woven polymer fibers have complex irregular air flow channels and no well defined pore

size. For these systems one speak about equivalent pore diameter which can be determined using the bubble-point test as described in Ref. [25].

Consider all percolating open channels through the filter. For each channel there will be a most narrow constriction. The equivalent pore diameter is a length characterizing the width of the biggest of all these most narrow constrictions[25]. It can also be considered as the diameter of the critical constriction as introduced in the theory of seals developed in Ref. [9–11]. In this theory the system is studied at increasing magnification or resolution. At the lowest magnification (say naked eye) the fiber mat appears as a homogeneous material and no leakage would be expected at this magnification. As we increase the magnification we observe some “big” cavity regions but they do not percolate so even at this magnification one would not expect any leakage. When we increase the magnification even more (say using an optical microscope) one finally observe for the first time an open percolating path. The critical constriction is the most narrow constriction along the first percolating path which can be observed with increasing magnification. The equivalent pore diameter is roughly the diameter of a circular hole with the same cross section area as that of the critical constriction.

Data Availability Statement: Data sharing is not applicable to this article as no new data were created or analyzed in this study.

-
- [1] A. Tcharkhtchi, N. Abbasnezhad, M.Z. Seydani, N. Zirak, S. Farzaneh, M. Shirinbayan, *An overview of filtration efficiency through the masks: Mechanisms of the aerosols penetration*, Bioactive Materials **6**, 106 (2021).
 - [2] Jeffrey T. Mueller, Soroor Karimi, Karl A. Poterack, Maria Teresa A. Seville, Steven M. Tipton, *Surgical Mask Covering of N95 Filtering Facepiece Respirators: The Risk of Increased Leakage*, Accepted Manuscript for Infection Control & Hospital Epidemiology as part of the Cambridge Coronavirus Collection. DOI: 10.1017/ice.2021.50
 - [3] A. Tiwari and B.N.J. Persson, *Physics of suction cup*, Soft Matter, 15(46), 9482 (2019)
 - [4] B. Lorenz, N. Rodriguez, P. Mangiagalli and B.N.J. Persson, *Role of hydrophobicity on interfacial fluid flow: Theory and some applications*, The European Physical Journal **E37**, 12 (2014).
 - [5] C. Yang, B.N.J. Persson, *Contact mechanics: contact area and interfacial separation from small contact to full contact*, J. Phys.: Condens. Matter **20**, 215214 (2008).
 - [6] A. Almqvist, C. Campan, N. Prodanov and B.N.J. Persson, *Interfacial separation between elastic solids with randomly rough surfaces: Comparison between theory and numerical techniques*, Journal of the Mechanics and Physics of Solids **59**, 2355 (2011).
 - [7] L. Afferrante, F. Bottiglione, C. Putignano, B.N.J. Persson, G. Carbone, *Elastic contact mechanics of randomly*

- rough surfaces: an assessment of advanced asperity models and Persson's theory*, Tribology Letters **66**, 75 (2018).
- [8] W.B. Dapp, A. Lücke, B.N.J. Persson, and M.H. Müser *Self-Affine Elastic Contacts: Percolation and Leakage* Phys. Rev. Lett. **108**, 244301 (2012).
- [9] B. Lorenz, B.N.J. Persson, *On the dependence of the leak rate of seals on the skewness of the surface height probability distribution* Europhysics Letters **90**, 38002 (2010).
- [10] B. Lorenz, B.N.J. Persson *Leak rate of seals: Effective-medium theory and comparison with experiment* The European Physical Journal E **31**, 159 (2010).
- [11] B.N.J. Persson, C. Yang, *Theory of the leak-rate of seals*, J. Phys.: Condens. Matter **20**, 315011 (2008).
- [12] *Comparison of FFP2, KN95, and N95 Filtering Face-piece Respirator Classes* 3M Science applied to life, Technical Bulletin, February 2021.
- [13] B.N.J. Persson, A. Kovalev and S.N. Gorb, *Contact Mechanics and Friction on Dry and Wet Human Skin* Tribology Letters volume **50**, 17 (2013).
- [14] A. Kovalev, K. Dening, B.N.J. Persson, and S.N. Gorb, *Surface topography and contact mechanics of dry and wet human skin*, Beilstein J Nanotechnol. **5**, 1341 (2014).
- [15] A CDC reports states that any presence of facial hair that gets in the way of a respirator mask's seal can cause 20 to 1000 times more leakage as compared to a clean-shaven mask-wearer. See: <https://blogs.cdc.gov/niosh-science-blog/2017/11/02/noshave/>
- [16] Julien van Kuilenburg, M.A. Masen and Emile van der Heide, *Contact modelling of human skin: What value to use for the modulus of elasticity?* Proc IMechE Part J:J Engineering Tribology **227**, 349 (2012).
- [17] S. Steve Zhou, Salimatu Lukula, Cory Chiossone, Raymond W. Nims, Donna B. Suchmann, M. Khalid Ijaz, *Assessment of a respiratory facemask for capturing air pollutants and pathogens including human influenza and rhinoviruses*, J. Thorac. Dis. **10**, 2059 (2018).
- [18] N. El-Atab, N. Qaiser, H. Badghaish, S.F. Shaikh, and M.M. Hussain, *Flexible nanoporous template for the design and development of reusable anti-COVID-19 hydrophobic facemasks*. ACS Nano **14**, 7659 (2020).
- [19] Z. Lei, J. Yang and Z. Zhuang, *Contact Pressure Study of N95 Filtering Face-piece Respirators Using Finite Element Method*, Computer-Aided Design & Applications **7**, 847 (2010).
- [20] A.J. Schaff, A.A. Ogale, *Tensile Viscoelastic Properties of Spunbonded Nonwoven Polypropylene Backing*, Textile Research Journal, 61, N, (1991).
- [21] A.B. Ihsan, T.L. Sun, T. Kurokawa, S.N. Karobi, T. Nakajima, T. Nonoyama, C.K. Roy, F. Luo, and J.P. Gong, *Self-Healing Behaviors of Tough Polyampholyte Hydrogels*, Macromolecules **49**, 4245 (2016).
- [22] JM Uruena, AA Pitenis, RM Nixon, KD Schulze, TE Angelini, WG Sawyer, *Mesh size control of polymer fluctuation lubrication in gemini hydrogels*, Biotribology **1**, 24 (2015).
- [23] J.P. Gong, *Friction and lubrication of hydrogels—its richness and complexity*, Soft Matter **2**, 544 (2006).
- [24] B.N.J. Persson, J. Guo *Electroadhesion for soft adhesive pads and robotics: theory and numerical results* Soft matter **15**, 8032 (2019).
- [25] W.G. Lindsley *Filter Pore Size and Aerosol Sample Collection*, CDC, NIOSH Manual of Analytical Methods, 5th Edition, Chapter FP, April 2016, Page FP-2 to FP-14.
- [26] See pages 233-235 in P.G. de Gennes, F. Brochard-Wyart and D. Quere, *Capillary and Wetting Phenomena: Drops, Bubbles, Pearls, Waves*, Springer, New York (2004)
- [27] D. Richard and D. Quere, *Bouncing water drops*, Europhysics Letters **50**, 769 (2000).
- [28] E.P. Vejerano and L.C. Marr, *Physico-chemical characteristics of vaporating respiratory fluid droplets*, J. R. Soc. Interface **15** 0939 (2017). <http://dx.doi.org/10.1098/rsif.2017.0939>
- [29] A. Einstein, *Über die von der molekularkinetischen Theorie der Wärme geforderte Bewegung von in ruhenden Flüssigkeiten suspendierten Teilchen [On the Movement of Small Particles Suspended in Stationary Liquids Required by the Molecular-Kinetic Theory of Heat]*. Annalen der Physik (in German) **322** 549 (1905).
- [30] B.N.J. Persson, *Adhesion between an elastic body and a randomly rough hard surface*, The European Physical Journal E **8**, 385 (2002).
- [31] B.N.J. Persson, I.M. Sivebäck, .N. Samoilov, K. Zhao, A.I. Volokitin, Z. Zhang, *On the origin of Amonton's friction law*, Journal of physics: condensed matter **20**, 395006 (2008).